BULLETIN OF THE EARTHQUAKE
RESEARCH INSTITUTE
UNIVERSITY OF TOKYO
Vol. 63 (1988) pp. 51-86

Seismic Structure and Formation of the Yamato Basin

Hiroshi KATAO

Earthquake Research Institute, the University of Tokyo

(Received April 28, 1988)

Abstract

Seismic refraction/reflection experiments were carried out in the Yamato Basin during the DELP-85 cruise. Twenty ocean bottom seismometers were deployed along two refraction lines crossing each other perpendicularly, namely Line A (230 km long trending NE-SW) and Line B (130 km long trending NW-SE). A large amount of explosives and a large volume airgum were used as sound sources.

Record sections of Line A and Line B are systematically different in both the cross-over distances of Pn and the distances of critical PmP arrival. To explain these differences, Pn anisotropy is required. In order to derive a precise seismic structure including lateral inhomogeneity, two-dimensional analyses were performed using ray tracing and synthetic seismograms. To satisfy both the gravity anomalies and the refraction data, the Moho must be shallower than 17.0 km, and almost flat along both Line A and Line B. When the Moho depth is assumed to be 16.5 km, the anisotropic Pn true velocities are 8.3 km/s for Line B and 7.65 km/s for Line A, respectively.

Although various seismic models of the Yamato Basin can be made to satisfy observed travel time patterns as well as amplitudes within the accuracy of 0.1 sec, a general feature of velocity distribution suggest that the crust of the Yamato Basin is classified into oceanic crust. However, the crustal thickness is 13-15 km which is almost twice as thick as that of the normal oceanic crust.

It is supposed that the drastic change of the paleomagnetic declination of the Japan Arc at about 15 Ma were mainly caused by the opening of the Yamato Basin. This abnormally thick crust of the Yamato Basin might be due to unknown petrological as well as kinematical processes induced by rapid opening of the basin.

1. Introduction

The origin and evolution of back arc basins is one of the most interesting problems in geophysics and geology today. Many studies have

been done on the tectonic process of back arc basin areas both theoretically and observationally. This subject is very important to understand the geological history of back arc-arc-trench systems.

Many ideas have been presented to explain the origin of back arc basins (ex. UYEDA and KANAMORI, 1979; TAYLOR and KARNER, 1983; MIYSHIRO, 1986). The most popular one is the back arc spreading, a process analogous to that in the ridge-transform system of midocean ridge regions. However, it seems that their origin and status at present are different in each basin, and many problems about the formation process are still unsolved. Therefore, the formation of the back arc basin was selected as one of main subjects of the DELP (Dynamics and Evolution of the Lithosphere Project).

The determination of the seismic velocity structure of crust and upper mantle is very important to understand the tectonics of back arc basins. The structure beneath a deep ocean basin is usually studied by seismic method using natural earthquakes as well as artificial seismic sources. However, seismological works have not been carried out sufficiently to study the structure of the back arc basin.

The Japan Sea is a back arc basin surrounded by the Japanese Islands Arc and the Asian continent. The Japan Sea is divided into three major basins: namely Japan Basin, Tsushima Basin and Yamato Basin. Many ideas have been presented about the origin of the Japan Sea: entrapment of the ocean, oceanization (BELOUSSOV, 1968), subsidence following upheaval and erosion (FUJITA, 1987), stable geosyncline (GNIBIDENKO, 1979) etc. However, it is generally believed that the Japan Sea was formed by the southward drift of the Japan Islands from the Asian continent (TERADA, 1934; MURAUCHI, 1971; MATSUDA and UYEDA, 1971 etc.). The opening process is still quite obscure on the basis of geological and geophysical evidence obtained from its basins.

Magnetic lineations are well defined in some back arc basins, for example the Mariana Trough and the Shikoku Basin (ex. KATAO *et al.*, 1985; BIBEE *et al.*, 1980; KOBAYASHI and ISEZAKI, 1976). However, the amplitude of the anomalies in the Japan Sea is small (100-300 nT) and its linearity is not clear. Especially in the Yamato Basin, it is difficult to recognize magnetic lineations (see Fig. 2 of ISEZAKI, 1986). Therfore, the opening mode and the age of the Yamato Basin cannot be defined by studies of geomagnetic anomalies. The linearity of the anomalies is clearer in the Japan Basin, and their linear pattern azimuth is NE-SW.

Some of the most important works about the origin and the formation

of the Japan Sea are studies of paleomagnetism. Paleomagnetic results suggest that the clockwise rotation of southwestern Japan and the anticlokwise rotation of northeastern Japan occurred in the post-Cretaceous (KAWAI *et al.*, 1971; YASKAWA, 1975). Recently, paleomagnetic measurements and fission track dating done by OTOFUJI *et al.* (1985) showed that the clockwise change of paleomagnetic declination took place during a very short period between 15 Ma and 14 Ma. Other geological and geophysical evidence suggests the opening of the Japan Sea during the Middle Miocene: for example a sharp changeover in molluscan faunas (CHINZEI, 1986), paleostress field (TAKEUCHI, 1986), abnormal arc volcanism (TAKAHASHI, 1986).

There are some seismic studies on the crustal structure of the Japan Sea (ANDREYAVA and UDINTSEV, 1958; MURAUCHI, 1972; LUDWIG *et al.*, 1975). Refraction methods using sonobuoys as well as the two-ship survey method have revealed that there is a systematic difference in structures between the Yamato Basin and the Japan Basin. It was shown that the Japan Basin seems to have a structure similar to that of typical oceanic basins. The Yamato Basin, however, was estimated to have a crust thicker than the Japan basin. The Pn velocity is about 7.6 km/s, which is about 5% lower than the avarage oceanic Pn velocity. Layer 2 is thicker because of a greater amount of 3.5 km/s capping material which is thought to be green tuff. It is not considered that the Yamato Basin has a characteristic features of normal oceanic basin. The Yamato Ridge, which is a topographic high dividing the Yamato Basin and the Japan Basin, was found to have a typical continental crust (MURAUCHI, 1966).

Analyses of surface waves across the Japan Sea have shown that the lithosphere thickness is about 30-40 km (ABE and KANAMORI, 1970; EVANS *et al.*, 1978). Land observations of a large explosion in the Japan Sea suggested the existence of Pn azimuthal anisotropy of about 5%, with highest velocity in the NW-SE direction (OKADA *et al.*, 1978).

Altough some seismic surveys have been carried out since the 1950's in the Japan Sea, refraction studies in the past were performed using the two-ship method or sonobuoy, and seismic structures were determined as classic layered models. Refraction study using new instumentation and analysis technique, for example use of ocean bottom seismometer (OBS), two dimensional ray tracing and synthetic seismogram, had not been carried out yet. Within the last decade, a new picture of the oceanic crust has emerged from these technical advances (SPUDICH and ORCUTT, 1980). In this new picture, it is important that velocity gradient, which cannot be

represented in the classical homogeneous layer model, characterizes the structure of the oceanic crust. Ray tracing and synthetic seismogram make it possible to construct a model including vertical velocity gradient and lateral heterogeneity.

2. Experiments

In the summer of 1985, as part of the Japanese Lithosphere Research Program (DELP: Dynamics and Evolution of the Lithosphere Project), geophysical and geological research cruises were made in the Yamato Basin and the Southeastern Japan Basin, southeast Japan Sea. The ship used for these cruises was the WAKASHIO-MARU chartered from Nippon Salvage Co. Ltd. During Leg I of DELP-85 cruises (July 15–28), a series of seismic refraction and reflection experiments was carried out to determine the precise seismic velocity structure of the crust and upper mantle of the Yamato Basin. The outline of DELP-85 cruises is summarized by the JAPANESE DELP RESEARCH GROUP ON BACK-ARC BASINS (1987).

For the seismic refraction survey, OBS's were used as receivers. Seismic refraction experiment using OBS can provide seismic records of high resolution, and are advantageous to determine the structure of the shallower part of the ocean crust as compared to the surface receivers. All the OBS's were free-fall and either transponder or timer triggered pop-up type instruments.

Twenty OBS's were deployed along Lines A and B at about 20 km interval distances. The longer NE-SW trending line (Line A) has a length of 230 km. The other NW-SE trending line (Line B) perpendicular to Line A has a length of 130 km, which is limited its length by the width of the basin (Fig. 1). One advantage in our experimental conditions as compared to previous studies is the length of the refraction lines. Especially, Line A has a length more than 200 km, which is long enough to determine the structure of the deeper part of the crust and uppermost mantle. If the refraction line length is less than 100 km, it is difficult to determine the Pn velocity of the Yamato Basin with high accuracy.

The seismic sources consisted of dynamite amounting to five tons in total weight and a large volume airgun. Dynamite explosions consisted of 154 shots (Fig. 2): ten large shots (300–500 kg) and 144 small shots (5, 10, 20 and 25 kg). Average spacing between successive shots is about 2.3 km. Locations of shots and OBS's were determined accurately by LORAN-C combined with NNSS navigation system. The dynamite shots were mainly used to constrain the deeper part of the crust and upper mantle structure.

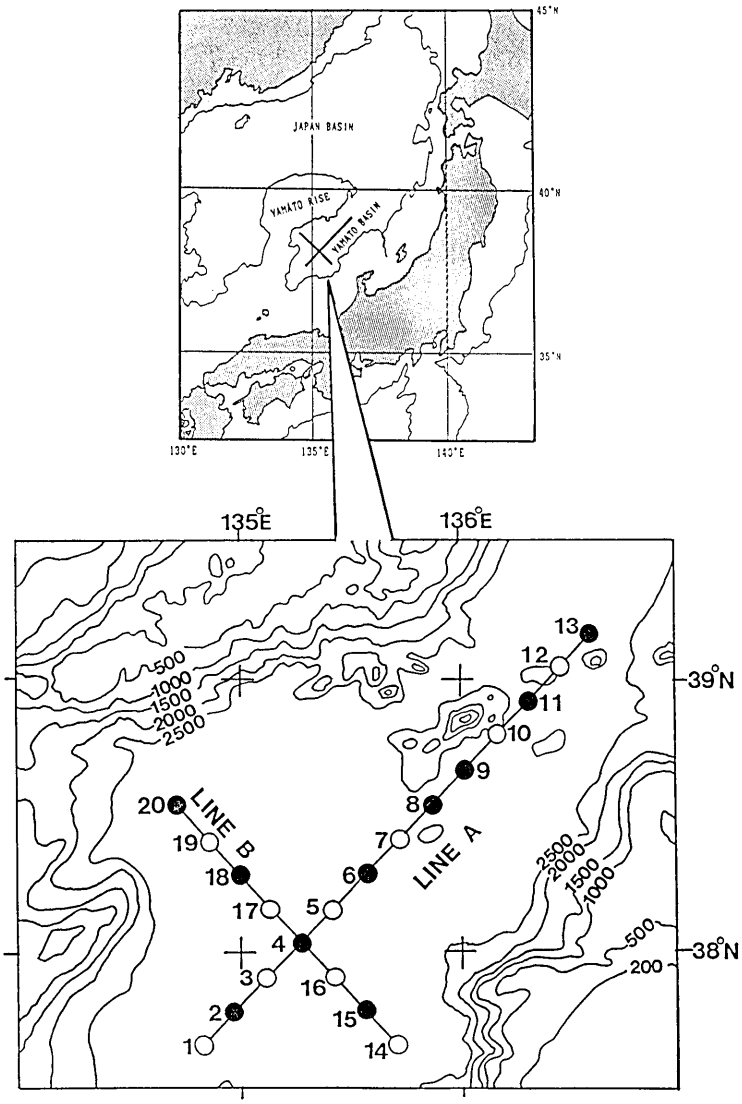

Fig. 1. (Above) Map of the Japan Sea and location of DELP-85 refraction experiment lines. (Below) Positions of OBS's and refraction lines. Solid circles represent OBS's of Earthquake Research Institute, University of Tokyo, and open circles represent OBS's of Geophysical Institute, University of Tokyo. Isobaths are in meters.

A large volume airgun (20 liters) was also used in determining the seismic structure in the shallower part of the crust along Lines A and B. Spacing between succesive shootings of the airgun was about 350 meters.

All of the OBS's were successfully retrieved after the operation (some

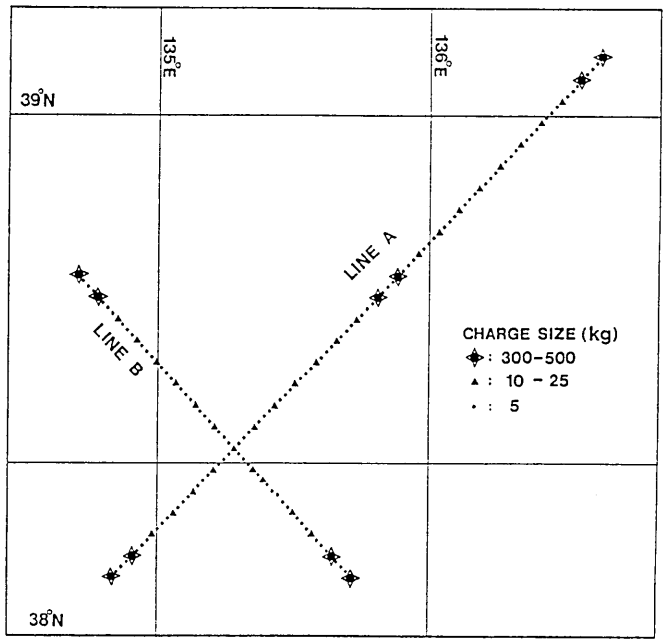

Fig. 2. Positions of dynamite explosions on DELP-85 refraction experiment.

were retrieved by the R/V TANSEI-MARU during Cruise KT85-15, September, 1985). Details of the refraction experiments are reported by HIRATA *et al.* (1987).

Multi-channel seismic profiling was also carried out on the same lines of seismic refraction experiments during DELP-85 cruises (TOKUYAMA *et al.*, 1987). The structure of the sediment layers and topography of the acoustic basement are obtained. Refraction survey combined with multi-channel profiler survey is effective to make a detailed model of the upper crust and to reduce ambiguity on determination of the lower structure (SUYEMASU, 1988).

3. Record Sections

3-1. Examples of Seismic Records

Examples of record sections obtained by the OBS's are presented below. All record sections are vertical components of geophone records without amplitude correction. The locations of OBS stations and dynamite shots are shown in Figs. 1 and 2. Structure analyses are performed for 16 OBS's. Four stations (YB-2, 8, 10 and 11) which failed to yield good seismic records are excluded from analyses.

i) YB-4 (Line A)

An example of the record section obtained at OBS station YB-4 is shown in Fig. 3. Station YB-4 was located at the cross point of two refraction lines. This panel is a record section of dynamite explosion along Line A with a reduction velocity of 8.0 km/s.

One main feature of this record section is such that the apparent velocity increases from about 4.0 km/s to 7.0 km/s at epicentral distance ranges of 10–50 km. The refracted wave from the mantle (Pn) is observed as the first arrival beyond about 80 km from the station. The apparent velocity of the Pn phase are 8.0 km/s or lower. The topography of the sea floor and acoustic basement along Line A are irregular due to the presence of many seamounts. Such undulation of the acoustic basement can be seen on the multichannel profiles (Fig. III-4 (a) of TOKUYAMA *et al.*, 1987). Because of the existence of seamounts and undulation of the basement, many irregularities of travel time are seen on the record section. Because undulation of the basement is hidden by the flat sediment surface, these irregularities cannot be cancelled by simple depth correction. Therefore, it is difficult to know exactly the true velocity of the uppermost mantle from only the observed record section. The true velocity cannot be estimated until two-dimensional modeling for the crust is performed. The waves reflected from the Moho discontinuity (PmP) arrive as later phases at the distance ranges 50–120 km. The critical reflection of the PmP which has the largest amplitude among the PmP phases arrives at about 50 km.

Figure 4 is a section of the airgun shooting record. The refracted waves from the basement have a velocity greater than 3.5 km/s.

ii) YB-9 (Line A)

The record section obtained from station YB-9 is shown in Fig. 5. This section consisted of seismic records of dynamite explosions along Line A. The apparent velocity of the first arrivals increases continuously up to distance of 80 km. The Pn phases are observed as a first arrival beyond 80 km, and their apparent velocity is less than 8.0 km/s. But exact apparent velocity cannot be estimated due to irregularities of travel times as in the case of station YB-4.

Figure 6 shows record section of airgun shooting. A line-up of first arrival with apparent velocity of 3.5 km/s is seen at distance range 6–9 km on the SW side of the station. Although irregularity due to undulation of basement topography is seen, the apparent velocity increases gradually with distance.

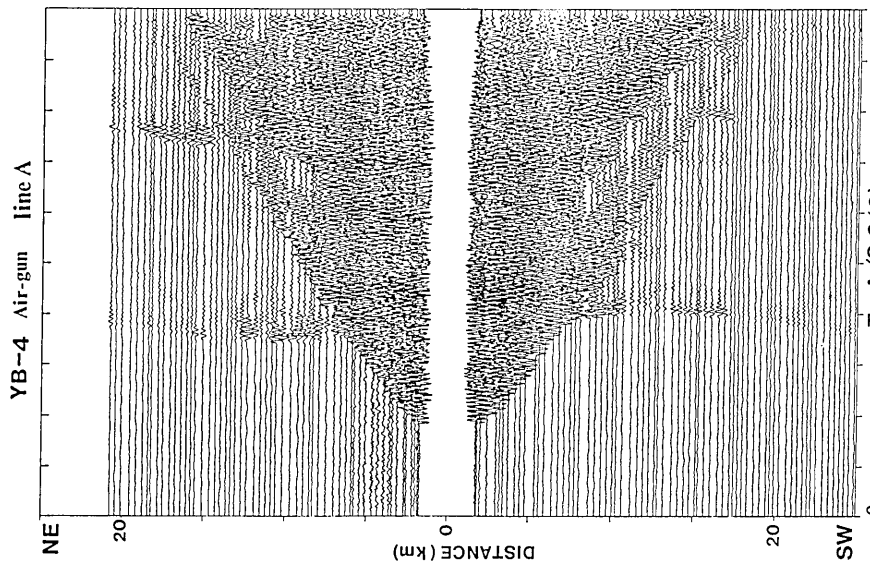

Fig. 4. Record section of airgun shooting along Line A for Station YB-4. Reduction velocity is 6.0 km/s. Low pass filter 30 Hz. Vertical component of geophone record.

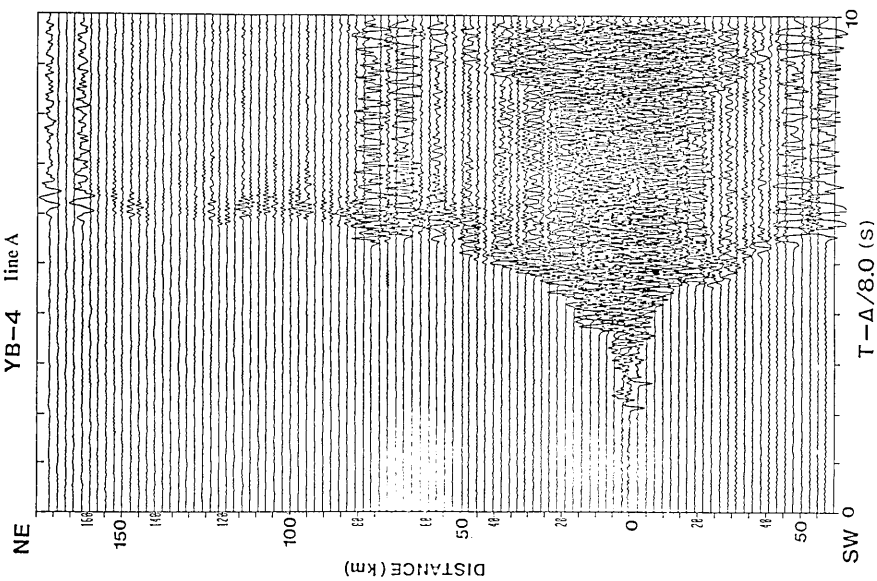

Fig. 3. Observed record section of dynamite explosions along Line A for Station YB-4. Reduction velocity is 8.0 km/s. Vertical component of geophone record. Low pass filter 20 Hz. No amplitude correction.

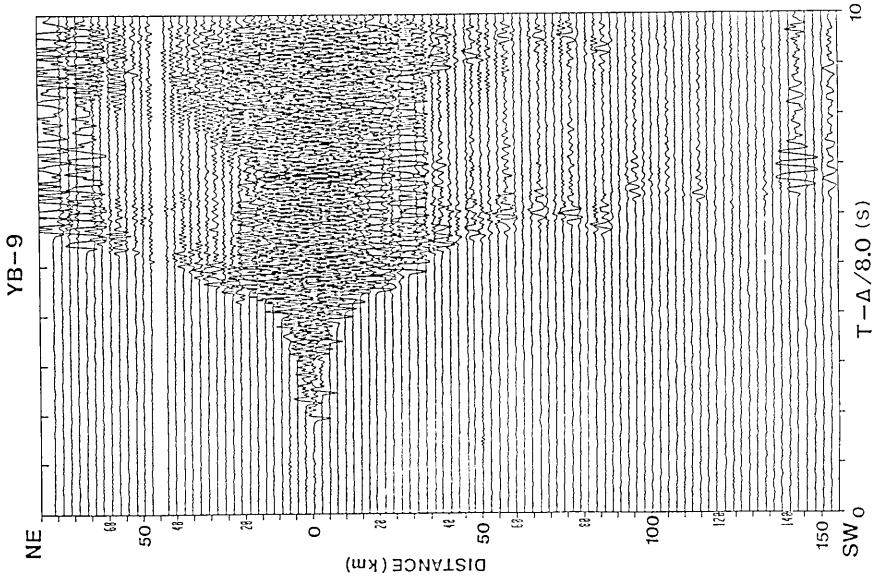

Fig. 5. Record section of dynamite shots along Line A for Station YB-9. Reduction velocity is 8.0 km/s. Low pass filter 15 Hz. No amplitude correction.

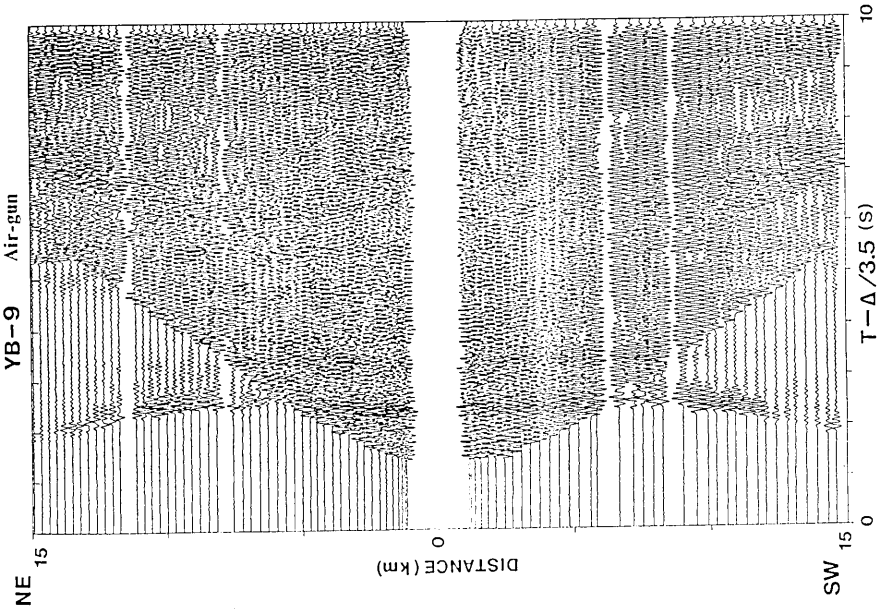

Fig. 6. Record section of airgun shooting along Line A for Station YB-9. Reduction velocity is 3.5 km/s. Low pass filter 30 Hz.

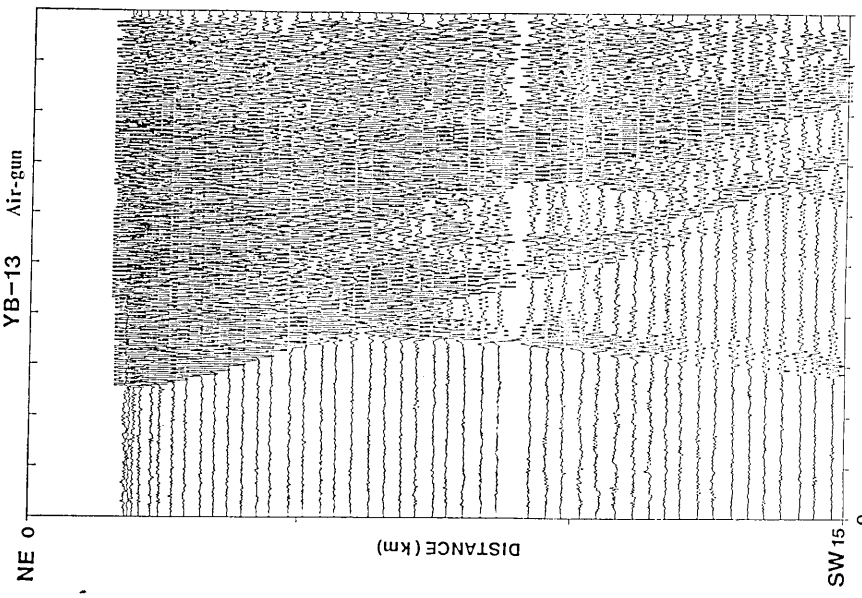

Fig. 7. Record section of airgun shooting along Line A for Station YB-13. Reduction velocity is 3.5 km/s. Low pass filter 30 Hz.

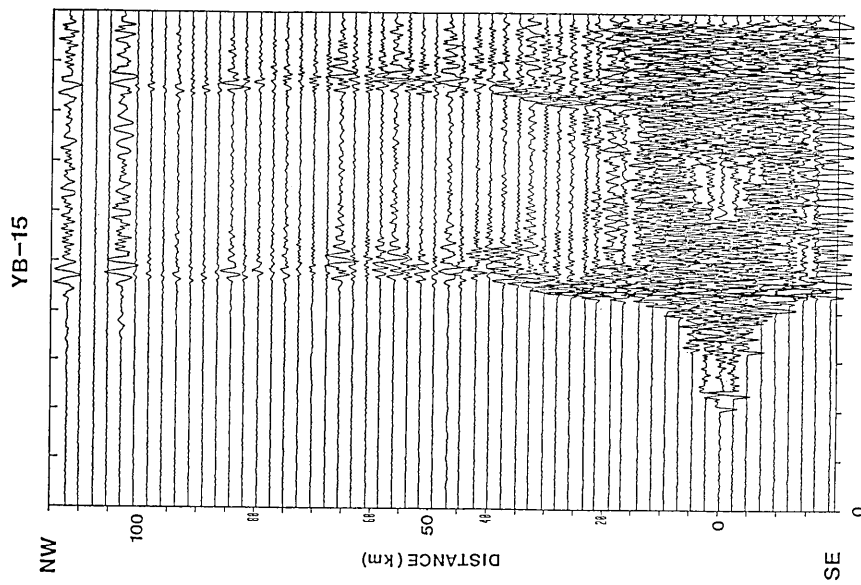

Fig. 8. Record section of dynamite explosions along Line B for Station YB-15. Reduction velocity is 7.0 km/s. Low pass filter 20 Hz. No amplitude correction.

iii) YB-13 (Line A)

Figure 7 is the airgun shooting record section obtained at Station YB-13 located at the NE end of Line A. A line-up of first arrival can be seen at distance range 5-8 km with very low amplitude. The apparent velocity of this phase is 3.5 km/s. The refracted later phases from sedimentary layer are seen with apparent velocity of 2.0 km/s just before the direct water wave arrivals.

iv) YB-15 (Line B)

The dynamite explosion record section along Line B obtained at Station YB-15 is shown in Fig. 8. The Pn phases can be seen beyond about 60 km with very low amplitude. The apparent velocity of Pn is much higher than 8.0 km/s, and estimated as 8.6 km/s. The refracted wave or diving wave from the lower crust is observed beyond 110 km with an apparent velocity of 7.0 km/s. The PmP phases have large amplitudes, and can be detected more clearly on Line B than on Line A. The critical PmP arrives at about 35 km from the station. The sea floor along Line B is almost flat, and the basement undulation is smaller than on Line A.

Fig. 9 shows record section of airgun shooting. It is clear that the apparent velocity increases gradually with distance. The later phase from sedimentary layer is seen with apparent velocity of 2.0 km/s or greater. No 3.5 km/s-layer is identified at this station.

v) YB-4 (Line B)

The record section of dynamite shots along Line B obtained at Station YB-4 is shown in Fig. 10. The apparent velocity of the first arrival increases continuously up to 7.0 km/s in the distance range of 5-30 km. The Pn phases become the first arrival beyond about 60 km. The PmP phase is observed more distinctly as compared with record sections along Line A. The critical reflection from the Moho is observed at distances of 35 km or nearer.

vi) YB-18 (Line B)

The dynamite shot record section along Line B obtained at Station YB-18 is shown in Fig. 11. The Pn phase is observed beyond 60 km as the first arrival. The apparent velocity of Pn is 8.1 km/s. The critical PmP is observed at a distance of 35 km.

Figure 12 is the airgun shooting record section. Later phase coming from the sedimentary layer is seen with the apparent velocity of 2.0 km/s. No 3.5 km/s-layer can be seen at this station.

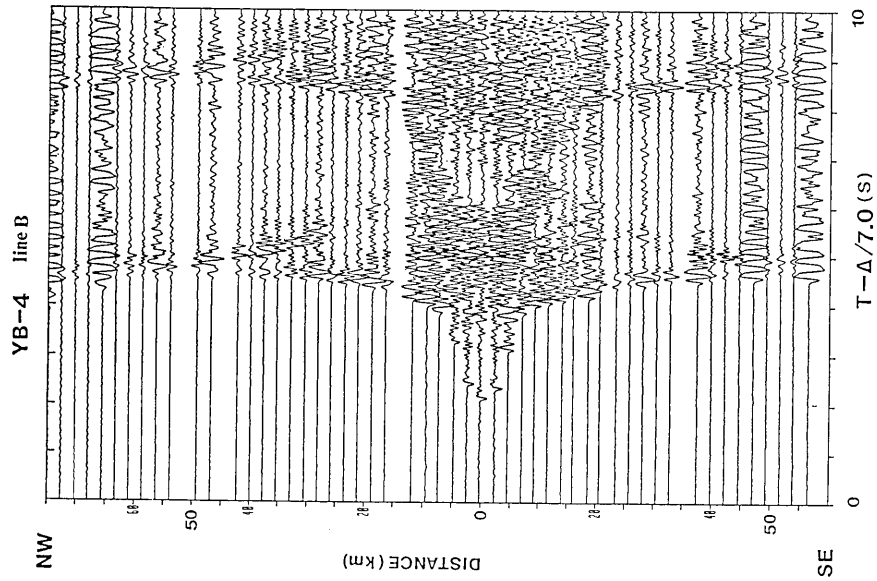

Fig. 10. Record section of dynamite explosions along Line B for Station YB-4. Reduction velocity is 7.0 km/s. Low pass filter 15 Hz. No amplitude correction.

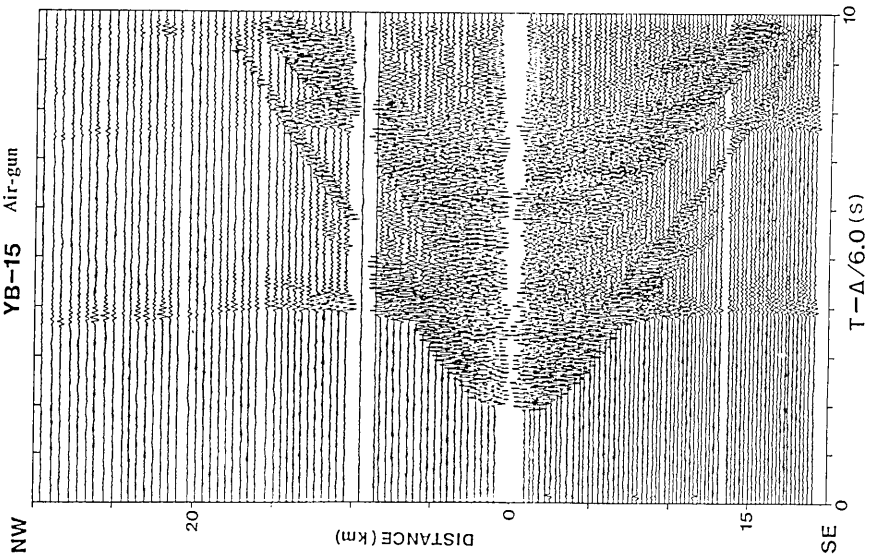

Fig. 9. Record section of airgun shooting along Line B for Station YB-15. Reduction velocity is 6.0 km/s. Low pass filter 30 Hz.

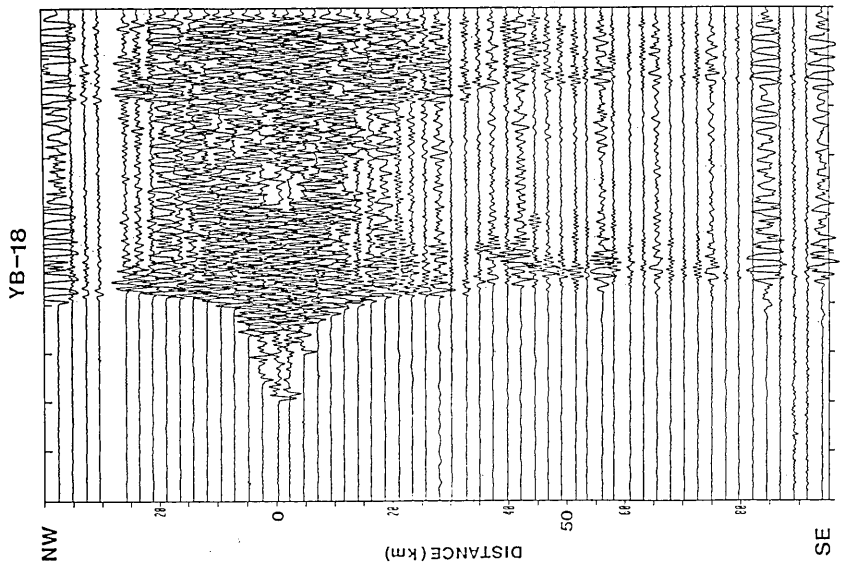

Fig. 11. Record section of dynamite explosions along Line B for Station YB-18. Reduction velocity is 7.0 km/s. Low pass filter 20 Hz. No amplitude correction.

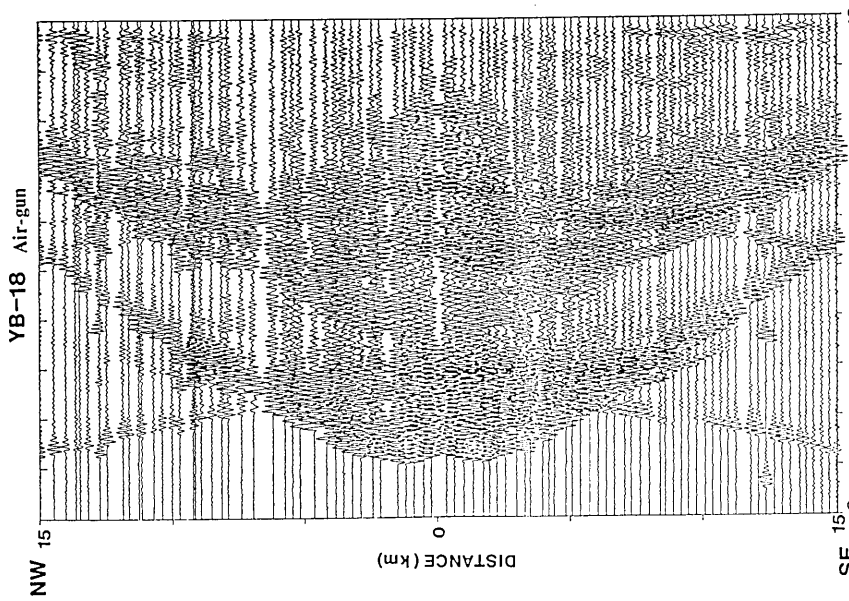

Fig. 12. Record section of airgun shooting along Line B for Station YB-18. Reduction velocity is 3.5 km/s. Low pass filter 30 Hz.

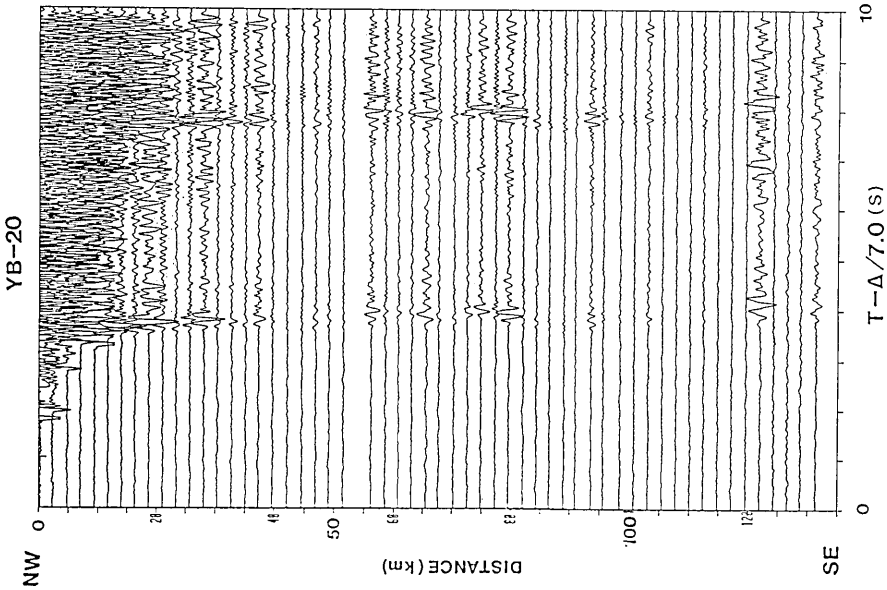

Fig. 13. Record section of dynamite shots along Line B for Station YB-20. Reduction velocity is 7.0 km/s. Low pass filter 15 Hz. No amplitde correction.

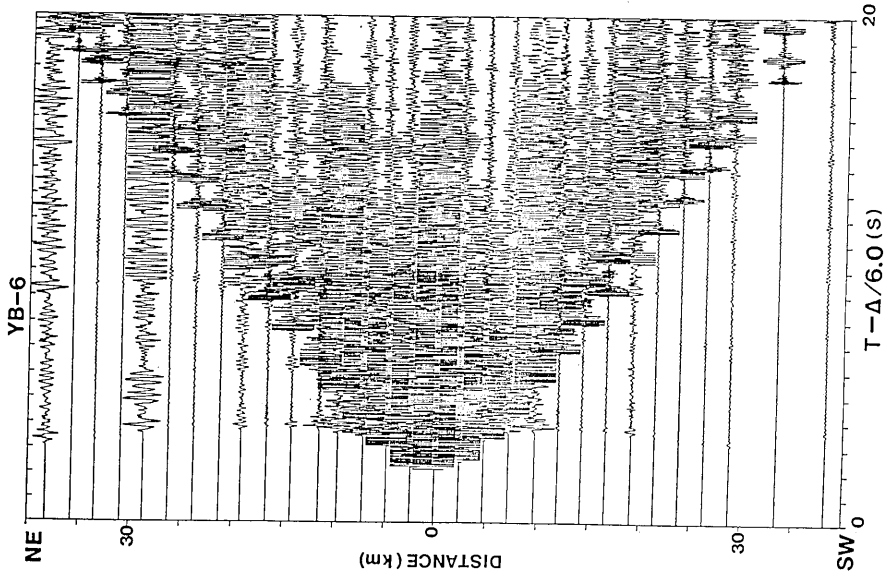

Fig. 14. Record section of dynamite shots along Line A for Station YB-6. This station is digital OBSH. Vertical component of geophone record. Reduction velocity is 6.0 km/s. No amplitude correction or digital filtering.

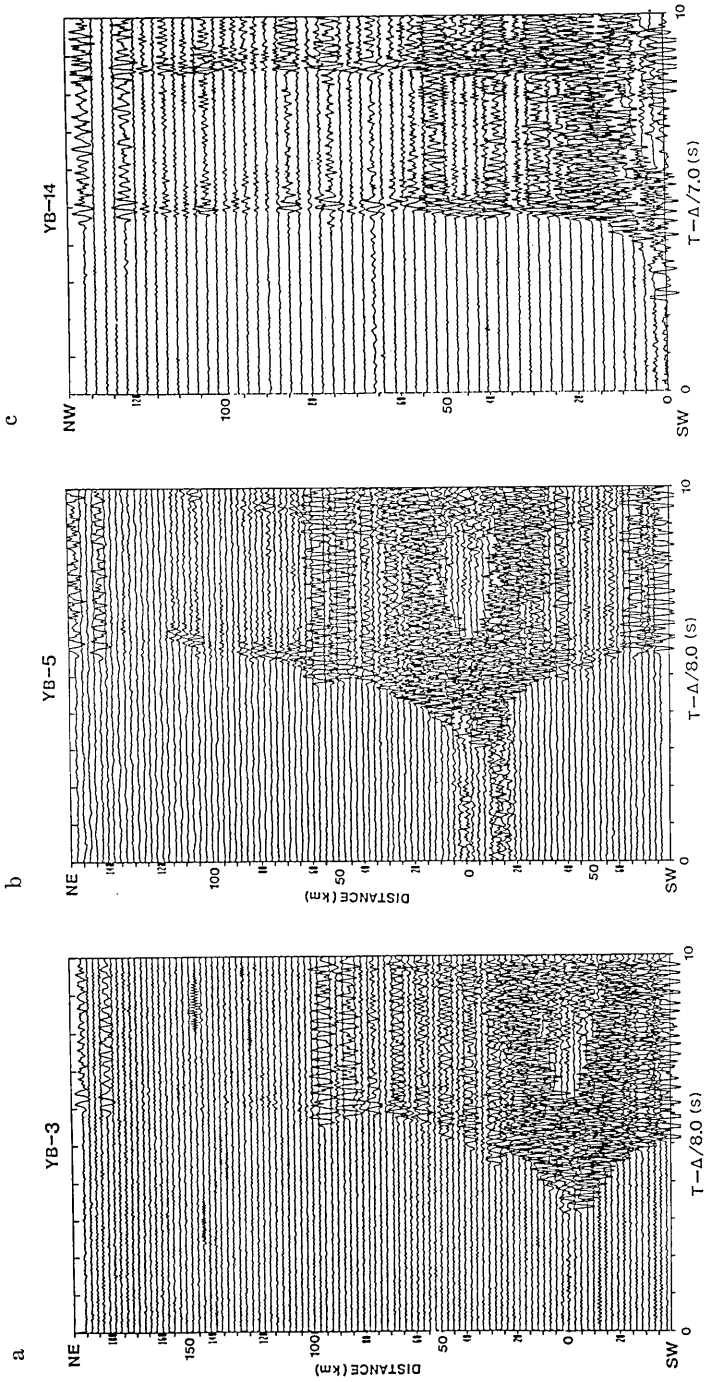

Fig. 15. (Left) Record section of dynamite shots along Line A for Station YB-3. (Middle) Record section of dynamite shots along Line B for Station YB-5. (Right) Record section of dynamite shots along Line B for the Station YB-14.

vii) YB-20 (Line B)

The record section of dynamite shots along Line B obtained at Station YB-20 is shown in Fig. 13. Station YB-20 is located at the NW end of Line B. The amplitude of the Pn phase is too small to be detected. The diving wave from the crust and PmP phase can be observed up to the southeastern end of the Line B.

viii) Other stations

The record section of dynamite shots along Line A obtained at Station YB-6 is shown in Fig. 14. This station is digital type OBS (KASAHARA *et al.*, 1985). As a feature of seismogram obtained by digital OBS, it can be seen that the S/N ratio and the dynamic range are higher than other OBS's of DAR (Direct Analogue Recording)-type. The arrival of the direct water wave is very sharp, and its amplitude is twenty times greater than the refracted wave. However, the shots of distant range were not recorded because the triggering parameters were not adequate.

Figure 15-a is a record section along Line A at Station YB-3. The Pn phase is observed as first arrival beyond about 80 km. The amplitude of the Pn from shots smaller than 10 kg is too small to be detected beyond 120 km except for the two large shots at the NE end of the line. Figure 15-b is the record section along Line A as Station YB-5. The Pn is seen at a distance beyond 80 km. The PmP is observed up to 120 km. Figure 15-c is the record section along Line B at Station YB-14. The PmP and the crustal refraction phases are observed up to the NW end of the Line B. The Pn is observed beyond 60 km with the apparent velocity of 8.3 kms. See HIRATA *et al.* (1987) for stations YB-1, 7, 12, 16, 17 and 19.

3-2. General Feature of Record Sections

The main features which can be extracted from figures above are now described.

a. Sediments

On the record sections of the 20 liters airgun at several stations (YB-4, 13, 15, 18), we can identify the refracted waves from velocity discontinuities in the sediments which appear as later phases with apparent velocities lower than 3.5 km/s.

b. Upper Crust

The refracted and reflected waves from the upper part of the crust appear at distances within 30 km from the stations. The appearance of these waves on the record sections differ from station to station. These irregularities are caused by regional variations of velocity structure in

the upper crust including topographic undulation of sea floor and the basement and thickness of the sediment layers.

It is commonly observed that the apparent velocity increases continuously with distance on the record sections. The high amplitude refracted waves from the basement are seen in the distance range of about 7–12 km with the apparent velocity of about 4.0 km/s or higher. Beyond it, the apparent velocity increases continuously from about 6.0 km/s to 7.0 km/s.

A line-up of the first breaks which have an apparent velocity of 3.5 km/s is identifiable in a couple of record sections from stations YB-9 and YB-13. However, no 3.5 km/s-layer is identified at the other stations.

c. Lower Crust

The refracted (diving) waves from the lower crust and reflected wave from the Moho discontinuity (PmP) can be observed on the record sections at all stations. The refraction phases from the lower crust appear as first breaks at distances beyond 30 km from the stations with apparent velocities around 7.0 km/s and can easily be traced up to the distance of about 130 km.

d. Pn and PmP

The apparent Pn velocities are 8.0 km/s or lower along the Line A. On the other hand, the apparent Pn velocities are higher than 8.0 km/s along Line B. These phases become the first arrivals beyond about 80 km for Line A and 60 km for Line B. The critical reflections from the Moho are observed at distances of about 50 km for Line A and around 35 km for Line B.

The appearance of the PmP amplitude and the Pn on record sections along Line A differ from station to station. These variations might be caused by the variation of the velocity transition between the lower crust and the uppermost mantle or local undulations on the Moho along Line A, besides the difference of the explosion charge size and effect of the shallower structure.

4. Structure Modeling

The preliminary results of this experiments were already reported by HIRATA *et al.* (1987) as follows: On the assumption of a flat-layered structure, the seismic velocity of the crust is similar to that for an oceanic crust. The Moho depth is around 18 km subsurface. Apparent Pn velocity is 8.0–8.1 km/s along both Lines A and B, and dose not show anisotropy.

In this paper, the author presents a more detailed seismic structure using two-dimensional analyses, and examines the preliminary results.

4-1. Existence of Pn anisotropy

At first, the structure of the crust and the uppermost mantle is determined by the classic method based on the slope of the line-up of the first arrival and its intercept time. The apparent Pn velocities observed on record sections have various values around 8.0 km/s. As a first approximation, an average velocity of 8.0 km/s is assumed for both Line A and B after HIRATA *et al.* (1987). Classical one-dimensional structure calculated for an isotropic mantle show that the depth of the Moho of stations on Line A differ systematically from those of the stations on Line B. The depth of the Moho discontinuity is around 20 km for stations along Line A, and are shallower for stations along Line B than those along Line A. Also, there are systematic differences in the cross-over distance of the Pn and the distance of the critical PmP as mentioned in Chapter 3. The Pn phases become first arrivals at distances beyond about 80 km along Line A, while the distances are beyond about 60 km along Line B. The critical PmP phases are observed at about 50 km along Line A, and at about 35 km along Line B. These distances are important parameters which depend on the depth and velocity contrast of the Moho. Therefore, it is clear that the seismic P-wave velocity of the topmost mantle is different along the two refraction lines, namely, lower along Line A, and higher along Line B. This situation implies the existence of P-wave anisotropy of the uppermost mantle, or lateral variations of the Pn velocity.

4-2. Two-Dimensional Modeling I ("Bowl-Shape" Model)

To derive a precise structure including the lateral inhomogeneity of the crust and uppermost mantle beneath the Yamato Basin, two dimensional analyses are performed using the ray tracing method and synthetic seismograms. Velocity models are constructed and refined by trial and error until calculated travel times coincide with the observed travel times within 0.1 sec.

The sediment layer structure and acoustic basement topography were taken from profiles of the multichannel reflection survey which was carried out on the same lines as the refraction experiments. The sediment layer is divided into two layers. The upper layer has a P-wave velocity of 1.6-1.8 km/s and the lower layer has a P-wave velocity of 2.0-2.2 km/s. These velocities are determined by the observed refracted wave from the sediment layers.

A P-wave velocity model in which Pn anisotropy is taken into consideration is constructed. The crust consists of three parts. The

velocity of the upper part of the crust is 4.0–5.0 km/s, and the velocity gradient is about 0.5 s^{-1}. The velocity model of the upper part is constructed based on record sections of the OBS-airgun refraction experiments. The seamounts can be represented by rising of the upper boundary of this layer (acoustic basement). The second part of the crust shows a velocity of 6.0–6.9 km/s with gradient of about 0.23 s^{-1}. The diving waves through this part are observed at distances of 10–30 km from the stations seen on the record sections. The velocity of the lower part of the crust is 6.9–7.2 km/s with gradient of about 0.038 s^{-1}. The P-wave velocity varies continuously at the boundary between the second part and lower part of the

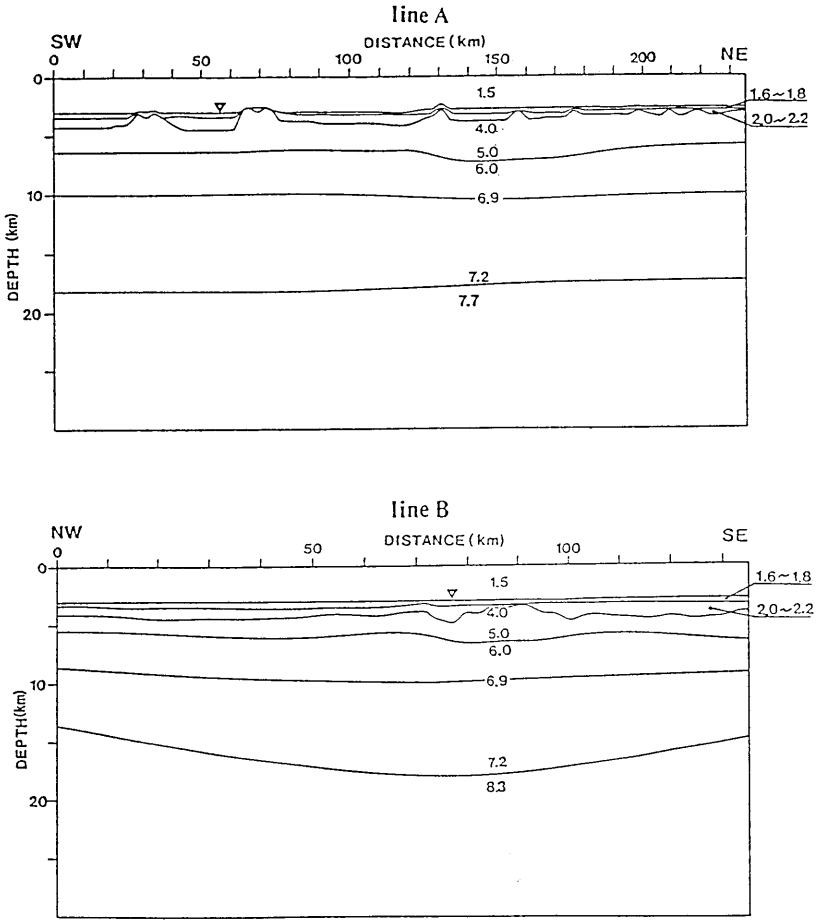

Fig. 16. "Bowl-shape" model: Model of P-wave velocity structure beneath the Yamato Basin. (Above) Line A. (Below) Line B. The Moho depth is 18 km at the crossing point (open triangle in figure) of both lines. Numerals represent P-wave velocity in km/s.

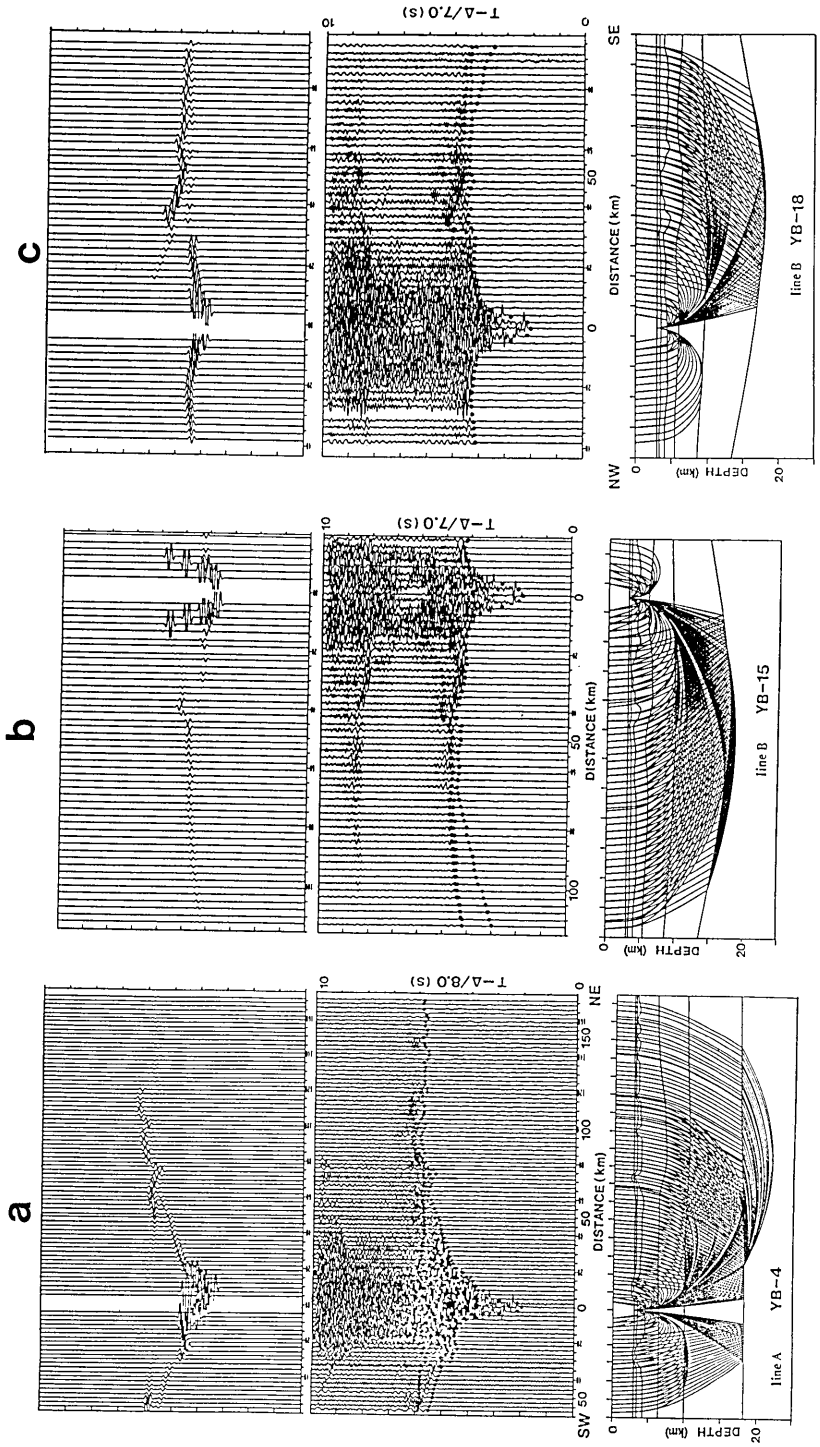

Fig. 17. Example of two-dimensional ray tracing based on model of Fig. 16 for Stations YB-4 (a) along Line A, and YB-15 (b) and YB-18 (c) along Line B. (Above) Synthetic seismogram. (Middle) Observed record section. Vertical component of geophone record. Amplitude correction due to dynamite charge weight. Dots represent theoretical travel times. (Below) Model and ray diagram.

crust, because the apparent velocity increases continuously from 6.0 km/s to 7.0 km/s without evident cusp on the record sections. The velocity gradient of the lower part of the crust is determined so as to satisfy such observations that diving waves through the lower crust and reflections from the Moho (PmP) reach 130 km along Line B and do not appear beyond about 130 km along Line A.

First, the Moho depth at the crossing point is taken as 18 km, which is an average of classic solutions of the two lines. Figure 16 shows this model. The true Pn velocities are 7.7 km/s for Line A and 8.3 km/s for Line B. The velocity gradient in the mantle is about 0.025 s^{-1}. The Moho discontinuity along Line B ascends toward the Yamato Rise and also toward the Honshu Island, and its deepest point is located at the center of the Yamato Basin. The shape of the Moho discontinuity is bowl-like.

Examples of ray tracing based on this model are shown in Fig. 17. Travel times are well fitted. Synthetic seismograms satisfy the amplitude features of the observed seismograms including the position of critical PmP arrival. Even though true upper mantle velocity is 7.7 km/s along Line A, the apparent Pn velocity of almost 8.0 km/s seen on the record section at station YB-4 is explained by sea floor topography, variation of sediment thickness and crustal structure.

To test the validity of this model, gravity data are used. The free air gravity anomalies around the Yamato Basin do not vary more than 20 mgal in the Yamato Basin (TOMODA, 1973). Theoretical gravity anomalies based on this velocity model along Line B is calculated by the method of TALWANI (1959) (Figs. 18 and 21). As shown on the calculated profile,

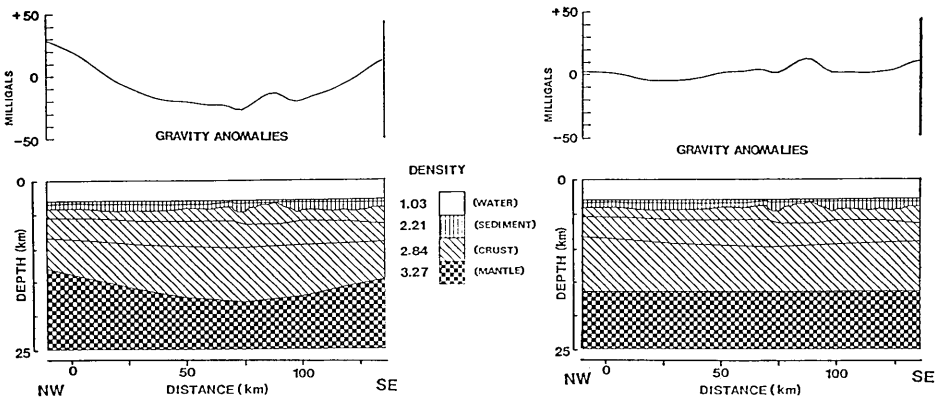

Fig. 18. (Left) Theoretical gravity anomalies calculated for the density model below based on the P-wave velocity model along Line B of Fig. 16. (Right) Theoretical gravity anomalies based on the velocity model along Line B of Fig. 19.

negative anomalies of more than 50 mgal exist at the center of the basin. Therefore, such a "Bowl-shape" model should be excluded.

4-3. Two-Dimensional Modeling II ("Flat" Model)

In order to construct a velocity structure which satisfies the gravity anomaly data, the depth of the Moho at the crossing point of two refraction lines is shallowed up to 16.5 km, and the shape of the Moho discontinuity is taken almost flat along Lines B and A (Fig. 19). Then, the P-wave velocity of the topmost mantle along Line A is reduced to 7.65 km/s, while that along Line B is kept at 8.3 km/s. The velocity gradient

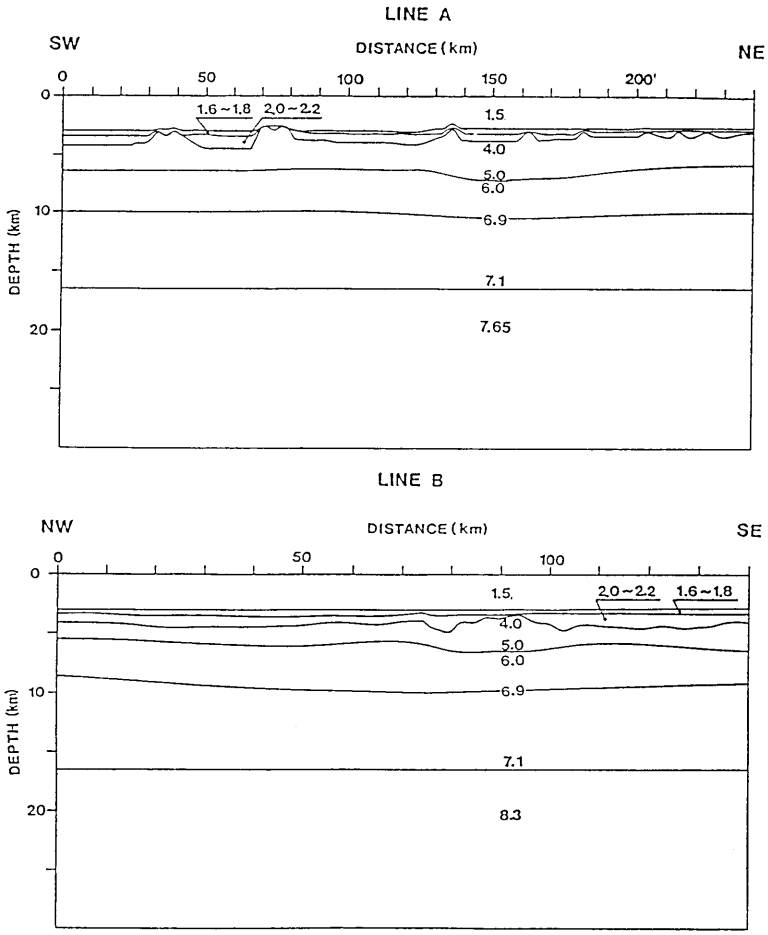

Fig. 19. "Flat" model: Model of P-wave velocity structure beneath the Yamato Basin. (Above) Line A. (Below) Line B. The Moho depth is 16.5 Km at the crossing point of both lines. Numerals represent P-wave velocity in km/s.

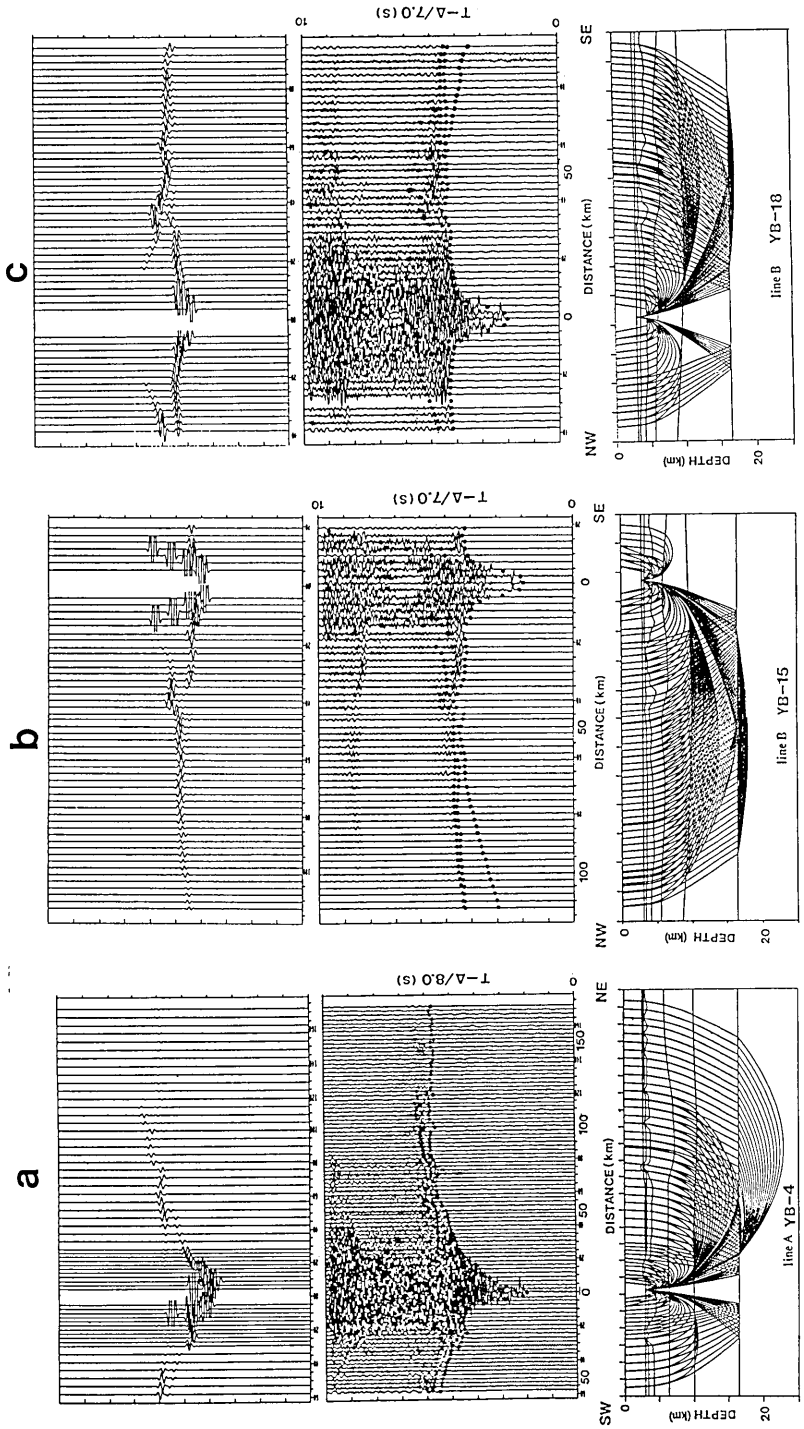

Fig. 20. Example of two-dimensional ray tracing based on model of Fig. 19 for Stations YB-4 (a) along the Line A, and YB-15 (b) and YB-18 (c) along Line B. (Above) Synthetic seismogram. (Middle) Observed record section. Vertical component of geophone record. Amplitude correction due to dynamite charge weight. Dots represent theoretical travel times. (Below) Model and ray diagram.

in the mantle is about 0.022 s^{-1}. The velocity gradient in the lower part of the crust is reduced slightly to 0.03 s^{-1} in order to fit the distance range at which the diving wave through the lower crust and PmP phases are observed. The structures of the uppermost crust and sediment layers are common with the model of Fig. 16.

Examples of ray tracing are shown in Fig. 20. Along Line A, the calculated travel times of the Pn phase match the observed travel times within the accuracy of 0.1 sec. The effect of shallowing of the Moho on travel times is canceled by reduction of the mantle velocity. The variation of the Pn phase slope is very small. Along Line B, the effect of flattening the Moho on the apparent Pn velocity is very small. The differences of PmP travel times and amplitudes as well as positions of the cusp of PmP are small between the two anisotropic models. It is almost impossible to find differences of seismograms between the "Flat" model and the "Bowl-shape" model.

The gravity anomalies caused by the "Flat" model are calculated (Figs. 18 and 21). The anomalies are almost flat except for regional anomalies with short wavelength and small amplitude less than 20 mgal due to seamounts, and satisfy the observed gravity anomalies. The density models and theoretical gravity anomalies which contain the adjacent area around the Yamato Basin are shown in Fig. 21. For precise comparison, the observed gravity anomalies are derived from the data base of the Ocean Research Institute, University of Tokyo (MAGBAT system), with accuracy

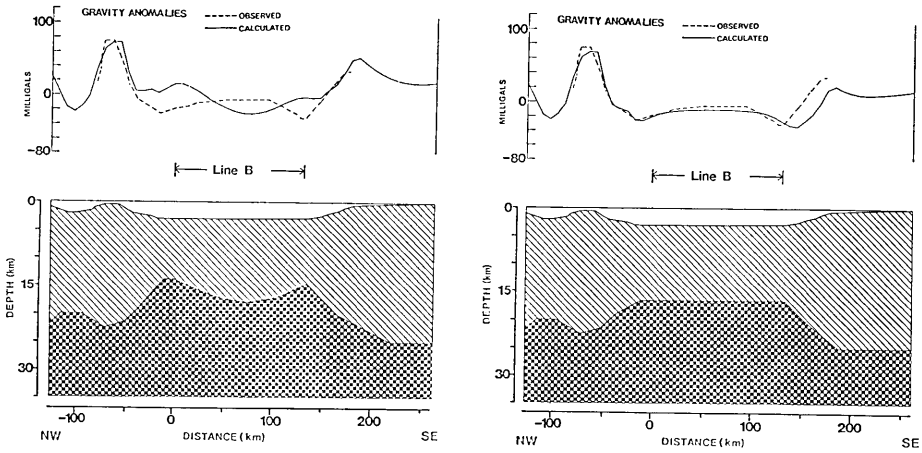

Fig. 21. (Left) Density model and theoretical gravity profiles along Line B for the Yamato Basin and its adjacent area based on the "Bowl-shape" model. Solid profile of the anomalies is calculated. Broken profile is observed. (Right) Density model and theoretical gravity based on the "Flat" model.

of 5 mgal. It is clear that the "Flat model" can explain in observed data very well.

4-4. Variation of Models

The seismic velocity models as stated above are not unique solutions, because the range of Pn anisotropy and the curvature of the Moho discontinuity could be variable. Six possible models along Line B are shown in Fig. 22. The differences of these models are depth and shape of the Moho, the Pn velocities, velocity gradient of the lower part of the crust. The structure of the upper part of the crust is common in all models. These models are equivalent for matching the calculated travel times to the observed seismograms within an accuracy of 0.1 sec.

4-6. Axial Low Velocity Zone Model

Among many possible models discussed above, the models which can satisfy the constraints given by gravity data require the P-velocity of the uppermost mantle along Line A to be 7.6–7.65 km/s. These velocities are nearly equal to the value which was proposed as "low mantle velocities" by LUDWIG *et al.* (1975). The P-wave velocity of 7.6 km/s may be too

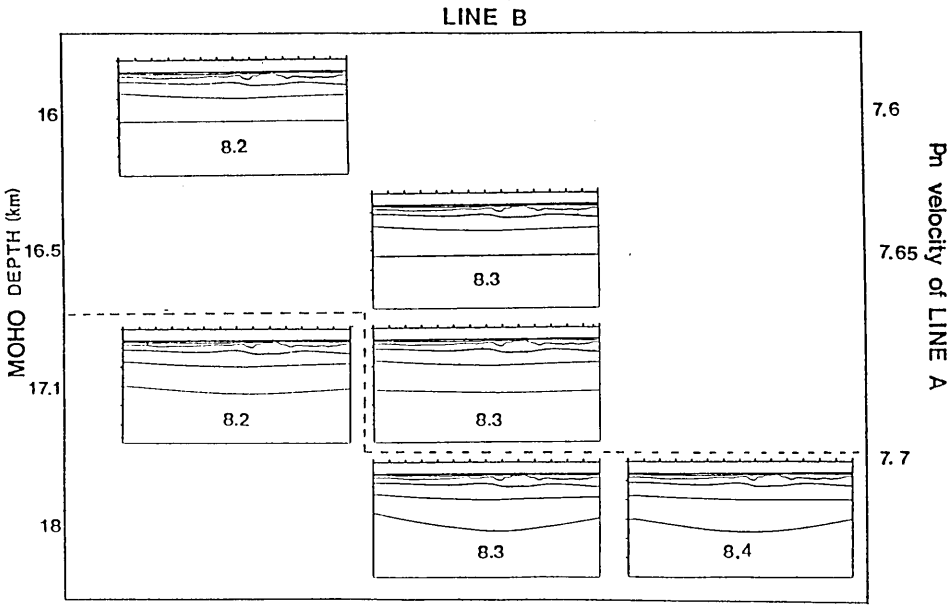

Fig. 22. Comparison of velocity structure models along Line B. Vertical axis at left is Moho depth. Vertical axis at right is Pn velocity of Line A corresponding with model of Line B. Numerals in models are Pn velocity along Line B.

low as a normal mantle velocity, even though anisotropy is considered.

This situation leads us to think that a zone of relatively low velocity mantle exist beneath the axial region of the Yamato Basin along Line A. After several trial-and-error calculations, a model in which the Moho is flat at the depth of 16.0 km subsurface was found (Fig. 23). The velocity distribution along Line B is such that the uppermost mantle velocity of 7.9 km/s at the crossing point of two refraction lines increases toward both sides of the crossing point, namely toward the margin of the basin, with the horizontal gradient of the velocity 0.015 s^{-1}, and becomes a constant velocity of 8.35 km/s at the distance of 30 km from the crossing

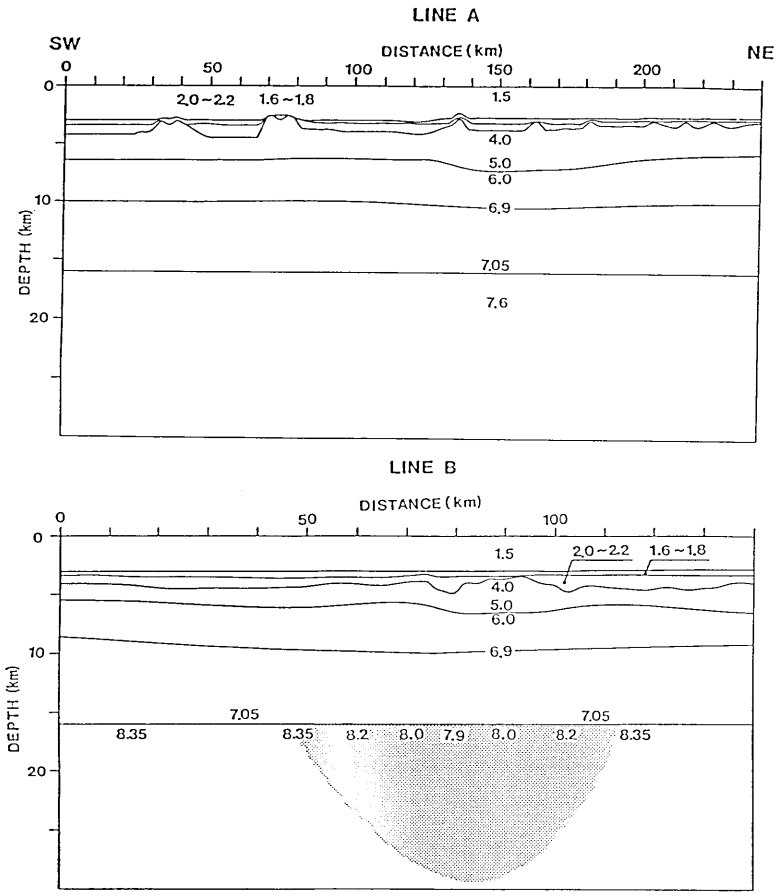

Fig. 23. Model of P-wave velocity structure beneath the Yamato Basin. (Above) Line A. (Below) Line B. The Moho depth is 16.0 km at the crossing point of both lines. Numerals represent P-wave velocity in km-s. Meshes on the model along Line B represent the low velocity region roughly.

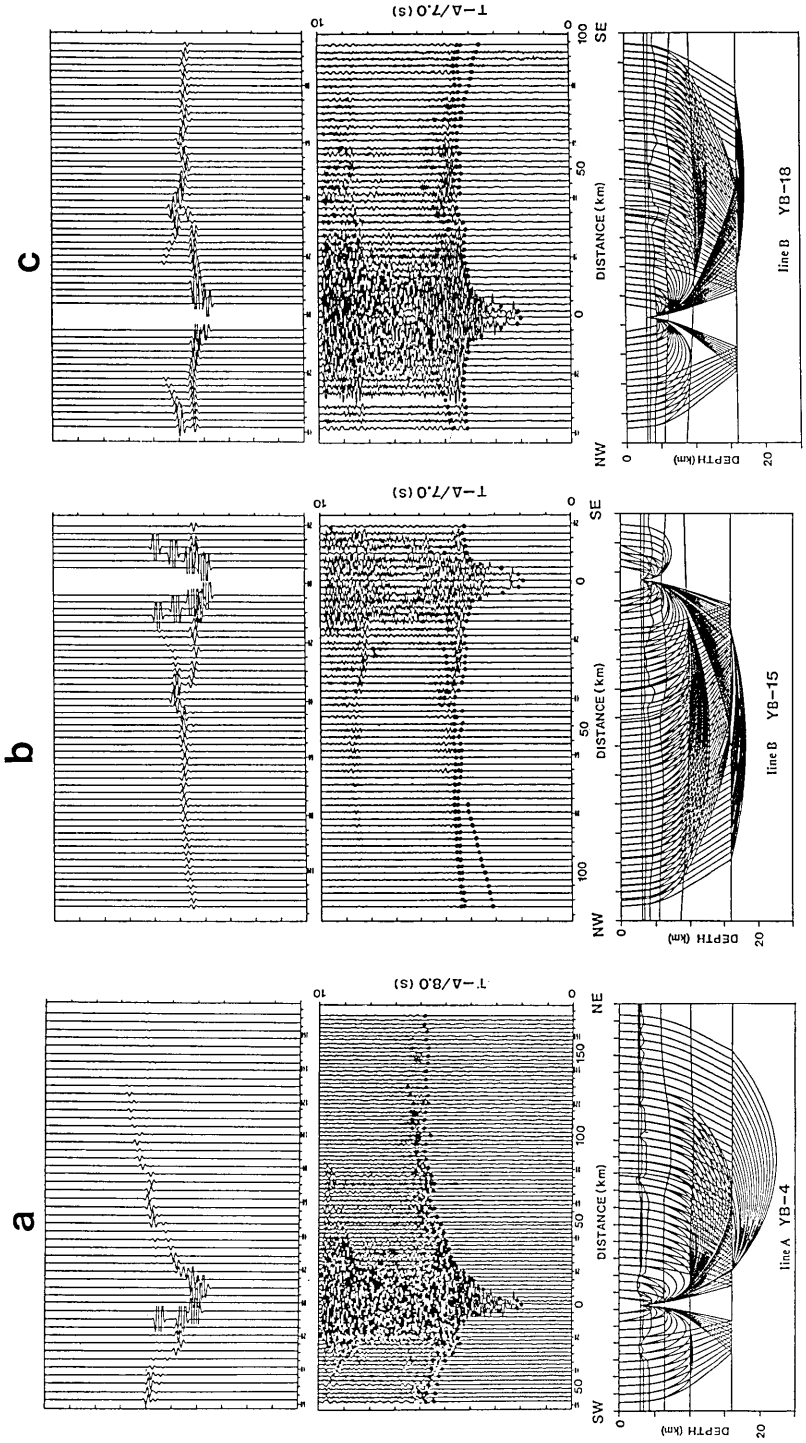

Fig. 24. Example of two-dimensional ray tracing based on model of Fig. 23 for Stations YB-4 along Line A (a), and YB-15 (a) and YB-18 (c) along Line B. (Above) Synthetic seismogram. (Middle) Observed record section. Vertical component of geophone. Amplitude correction due to dynamite charge weigh. Dots represent theoretical travel times. (Below) Model and ray diagram.

point, and keeps the same value far beyond. The Pn velocity along Line A has a constant value of 7.6 km/s. The Pn anisotropy becomes about 3% at the center of the basin. Examples of ray tracing are shown in Fig 24. As seen in figures, the fittings for both the travel times and the amplitude patterns are good.

This model is only an example of the axial low velocity models. The Pn velocity of 7.9 km/s at the center of Line B is the minimum value which can match the observed data, and can be increased to 8.0 km/s or higher. Many variations of axial low velocity model might be constructed by modification of parameters such as the low velocity zone width, the Moho shape and Pn velocity at the center of the basin.

5. Discussion

5-1. Variety of Models

In Chapter 4, it is shown that various models can exist for the structure of the lower crust and the uppermost mantle of the Yamato Basin. In these models, which are shown in Fig. 22, the Moho depth must be well constrained by the travel times of PmP at a short range from the station. However, the differences of the calculated travel times of PmP for these models are very small in the range where PmP phases are identifiable. This is because the PmP phases are observed as later phases and reduce their amplitudes rapidly in the sub-critical reflection region. Therefore, significant differences between these models cannot be identified on the record sections within the accuracy of 0.1 sec.

Such a model that has a Moho depth deeper than 18 km should be excluded, because the Moho curvature and/or the Pn velocity which satisfies the observed data becomes too large to be realistic. A model which has a Moho depth shallower than 16 km should also be excluded, because the Pn velocity along Line A is required to be too low.

The models shown below the broken line in Fig. 22 result in gravity anomalies of amplitude more than 20 mgal. Therefore, these models cannot satisfy the gravity observations data in the Yamato Basin.

In addition to the above anisotropic models, we found that a model can exist which has a low velocity zone in the upper mantle beneath the axial region of the Yamato Basin. This model can meet other geological and geophysical features observed in the basin. Many seamounts and knolls form a seamount chain along Line A. Ages of these seamounts are determined to be 6-12 Ma by the potassium-argon method (KANEOKA, 1986; KIMURA *et al.* 1987). Magnetic survey around these seamounts concluded

that the magnetic declination of these seamounts are nearly N-S, and the seamounts were formed at the present location (SAYANAGI *et al.*, 1987). It is supposed that these seamounts were formed in the latest stage of basin formation or in the period of several million years younger than it. These observation suggests that a region of high temperature related to formation of the basin and the seamount chain still remains beneath the axis region of the Yamoto Basin.

However, it is considered that the Yamato Basin is not active at present, because no shallow earthquake has been observed in this region. The OBS's used for the DELP-85 experiments did not detect any micro-seismicity at all during the observation period of more than two weeks.

In the case of the axial low velocity zone model of Fig. 23, Pn anisotropy of 3% still exists in the axial region of the basin. The difference of Pn velocity of the two refraction lines cannot be explained by only the regionality of Pn velocity. The existence of such low velocity mantle should be examined by further analyses of geophysical and petrological data.

5-2. General Feature of Seismic Structure

i) Crustal Structure

The vertical trend of P-wave velocity variation in the crust is similar to that of typical oceanic crust. An average crustal structure as a representative of the models stated in Chapter 4 is shown in Fig. 25. The upper part of the crust underlying the sediment layers is a region of high velocity gradient (0.2-0.5 s^{-1}) in which the velocities increase from about 4.0 to 6.9 km/s. The lower part of the crust has velocities of 6.9-7.2 km/s, and is characterized by a small velocity gradient (0.025-0.038 s^{-1}). These models do not have the predominant 6.0 km/s-layer which is generally

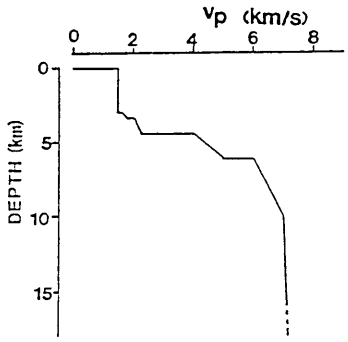

Fig. 25. Average P-wave velocity structure of the crust beneath the Yamato Basin.

observed in continental regions. The uppermost part of the crust corresponds to oceanic Layer 2 of classic layered models (ex. RAITT, 1963 ; SHOR *et al.*, 1970) and the lower crust correspond with the oceanic Layer 3. The part of the crust where the velocity increases from 6.0 to 6.9 km/s may be a transition zone between Layers 2 and 3.

LUDWIG *et al.* (1975) reported that Layer 2 is thicker than the normal oceanic crust because of a greater amount of 3.5 km/s capping material in the Yamato Basin. This 3.5 km/s-layer is thought to represent a wide range of consolidated sediments and volcanics (green tuff). However, in this study, the apparent velocity of 3.5 km/s could not be found except for some ambiguous line-ups. It is likely that the 3.5 km/s layer either does not exist at all or is limited regionally in a small area, namely, the northeastern region of the basin where the line-up of 3.5 km/s is observed by stations YB-9 and YB-13.

ii) Thickness of the Crust

The Moho discontinuity exists at a depth of 16–18 km from the surface. Excluding water layer of about 3 km thick, the crustal thickness is 13–15 km. This is greater than the normal oceanic crust, namely, twice as thick as that of the normal oceanic crust.

iii) Pn Anisotoropy

Pn anisotropy exists in the uppermost mantle beneath the Yamato Basin: a higher velocity along the NW-SE direction and a lower velocity along the NE-SW direction. The magnitude of the Pn anisotropy is 6–9%, which is greater than the value of 5% proposed by OKADA *et al.* (1978). Our data are less biased by lateral inhomogeneity, because the survey area was limited only in the deep basin region not including any continental crust area. The existence of Pn anisotropy suggesst that the lithosphere of Yamato Basin was formed through a similar process to spreading at the midoceanic ridges, and its direction was NW-SE.

5-3. Comparison with Other Regions

The gradient of the velocity structure of the Yamato Basin is similar to that of the typical oceanic basin, and clearly differs from that of a stretched continental crust which has a prominent 6.0 km/s-layer as seen in the North Sea (BARTON and WOOD, 1984) and the Okinawa Trough (NAGUMO *et al.*, 1986).

The crustal thickness of the Yamato Basin, however, is almost twice as thick as that of a typical ocean basin. On the other hand, other back arc basins, such as the Shikoku Basin, the West Philippine Basin (MURA-

UCHI *et al.*, 1968), the Palace Vela Basin (MOROZOWSKI and HAYS, 1979) and the Mariana Trough (BIBEE *et al.*, 1980), have an oceanic crust with normal thickness. Therefore, from the criterion about the crustal thickness, the Yamato Basin could not be regarded as a typical oceanic crust, and is different from back arc basins of oceanic type.

A similar abnormal thick oceanic crust is reported in the regions of oceanic plateaus (CARLSON *et al.*, 1980). These plateaus which have crustal thickness of 10–40 km clearly differ from continental fragments with respect to seismic velocity structure: for example the Tuamotu Plateau (TALANDIER and OKAI, 1987), Eauripik-New Guinia Rise (DEN *et al.*, 1971), Hawaiian Ridge (WATTS *et al.*, 1985).

The continent-ocean transition zone at many passive margins also has very thick sequences of basaltic igneous rocks (MUTTER *et al.*, 1988). The crust of the Yamato Basin might consist of only these transition zones because of the short basin width.

5-4. Formation of the Yamato Basin

The ages, crustal structure and other observations of the Yamato Basin and the Japan Basin suggest that the period and proccess of the formation are different between these two basins. Although paleomagnetic studies suggest that the opening of the whole Japan Sea occurred in "double door opening mode" during a very short period arround 15 Ma (OTOFUJI *et al.*, 1986), the whole Japan Sea cannot be considered to have been formed by single event. This is because the crustal structure of the Yamato Basin is different from that of the Japan Basin which has a crust similar to normal oceanic crust (LUDWIG *et al.*, 1975). Potassium-argon ages of rock samples dredged from the Japan Basin are older than 15 Ma and those from the Yamato Basin (KANEOKA, 1986). Age estimates based upon the basement depth, sediment stratigraphy and heat flow suggest an age difference between the Japan Basin and Yamato Basin (HILDE and WAGEMAN, 1973; TAMAKI, 1986). CELAYA and MCCABE (1987) propose a two-stage opening event for the Japan Sea.

The drastic change of magnetic declination found by OTOFUJI *et al.* (1985) could be interpreted simply as such that the rotation of the southwestern Japan occurred at the period of about 15 Ma. It is possible that the opening of the Japan Basin occurred prior to 15 Ma by almost parallel drift not accompanied by change of magnetic declination of the Honshu Island. In this case, the rotation of southwestern and northeastern Japan was related to only the opening of the Yamato Basin (Fig. 26). To

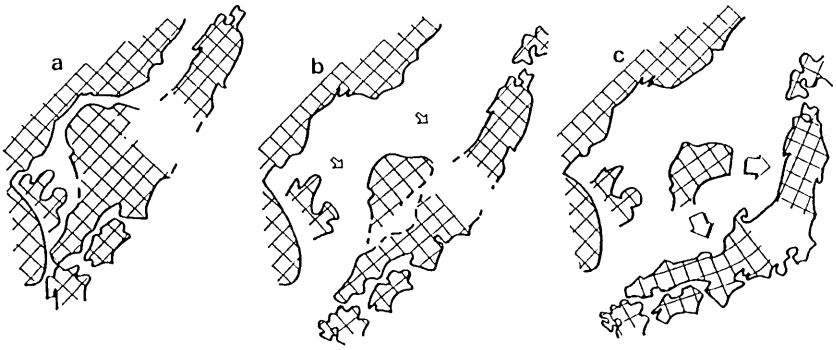

Fig. 26. Schematic illustrations of two-stage opening of the Japan Sea. (a) Before opening of the Japan Sea. (b) After spreading of the Japan Basin. (c) After opening of the Yamato Basin (present position).

explain the change of paleomagnetic declinations only by the opening of the Yamato Basin, the pivot of rotation for southwestern and northeastern Japan must be located nearer to the Yamato Basin than the poles proposed by OTOFUJI *et al.* (1986).

If we think that the Japan Basin could have opened by almost parallel drifting of the Honshu Island through a normal spreading process with relatively slow spreading rate, it is probable that the quick rotations of northeastern and southwestern Japan were caused only by rapid opening of the Yamato Basin. If the timing of the rotation determined by OTOFUJI *et al.* (1985) is valid, the opening of the Yamato Basin began at 15 Ma and terminated within one million years. Such a rapid opening, probably more than 20 cm/year, is not observed in the midocean ridge regions at present. These rapid opening processes of the Yamato Basin should be induced by change of plate motion as well as subduction mode which occurred at nearly the same time around the Japanese Islands Arc, such as opening and termination of the Shikoku Basin and arc collision in Hokkaido.

Although thickness of typical oceanic crust is relatively uniform and independent of age (MCCLAIN and ATALLAH, 1986) except for active mid-oceanic ridge regions, the crust of the Yamato Basin is abnormally thick. Crustal formation during rapid opening of the Yamato Basin might have been different from the normal midoceanic ridge type, and resulted in abnormal thickness of the crust.

Acknowledments

I would like to express sincerely thanks to Prof. S. Nagumo for giving me valuable suggestions and support. I thank Mr. S. Koresawa for his

encouragement. I wish to express my thanks to Dr. N. Hirata for providing the records of OBS's which belong to the Geophys. Inst., Univ. of Tokyo, for this study. Dr. H. Tokuyama and Mr. M. Suyemasu gave me the multi-channel profile on the DELP1985 cruise. Drs. K. Tamaki, K. Kimura and Mr. Sayanagi provided me with the gravity anomaly data of MAGBAT or JNOC. Mr. A. Kubo and Miss K. Kondo helped in final preparation of this manuscript.

References

ABE, K. and H. KANAMORI, 1970, Mantle structure beneath the Japan Sea as revealed by surface waves, *Bull. Earthq. Res. Inst., Univ. Tokyo*, 48, 1011-1021.

ANDREYEVA, I. B. and G. B. UDINTSEV, 1958, Bottom structure of the Sea of Japan according to data obtained by the research ship Vityaz, *Izv. Akad. Nauk USSR, Ser, Geol.*, **10**, 3-20 (in Russian).

BARTON, P. and R. Wood, 1984, Tectonic evolution of the North Sea basin: crustal streching and subsidence, *Geophys. J. R. astr. Soc.*, **79**, 987-1022.

BELOUSSOV, V. V., 1968, Some ploblems of development of the earth's crust and upper mantle of oceans, in The crust and upper mantle of the Pacific area, Geophys. Monogr. Ser., 12, ed. by L. Knopoff et al. AGU, Washington D. C., pp. 449-459.

BIBEE, L. D., G. G. SHOR JR. and R. S. LU, 1980, Inter-arc spreading in the Mariana Trough, *Mar. Geology*, **35**, 183-197.

CARLSON, R. L., N. I. CHRISTENSEN and R. P. MOORE, 1980, Anomalous crustal structure in Ocean Basins: continental fragments and oceanic plateaus, *Earth Planet. Sci. Lett.*, **51**, 171-180.

CELAYA, M. and R. MCCABE, 1987, Kinamatic model for the opening of the Sea of Japan and the bending of the Japanese islands, *geologh*, **15**, 53-57.

CHINZEI, K., 1986, Opening of the Japan Sea and marine biogeography during the miocene, *J. Gemag. Geoelect.*, 38, 487-494.

DEN, N., W. J. LUDWIG, S. MURAUCHI, M. EWING, H. HOTTA, T. ASANUMA, T. YOSHII, A. KUBOTERA and K. HAGIWARA, 1971, Sediments and structure of the Eauripik-New Guinea Rise, *J. Geophys. Res.*, **76**, 4711-4723.

EVANS, J. R., K. SUYEHIRO and I. S. SACKS, 1978, Mantle structure beneath the Japan Sea—a re-examination, *Geophys. Res. Lett.*, **5**, 487-490.

FUJITA, Y., 1987, The origin of the Japan Sea, *Chikyu*, **9**, 256-267 (in Japanese).

GNIBIDENKO, H., 1979, The tectonics of the Japan Sea, *Mar. Geol.*, 32, 71-87.

HILDE, T. W. C. and J. M. WAGEMAN, 1973, Structure and origin of the Japan Sea, The Western Pacific-Island arcs, Marginal Seas, Geochemistry, ed. by P. J. Coleman, Univ. Western Australis Press, pp. 415-434.

HIRATA, N., H. KINOSHITA, K. SUYEHIRO, M. SUYEMASU, N. MATSUDA, T. OUCHI, H. KATAO, S. KORESAWA and S. NAGUMO, 1987, Report on DELP 1985 cruise in the Japan Sea part II: Seismic refraction experiment conducted in the Yamato Basin, southeast Japan Sea, *Bull. Earthq. Res. Inst., Univ. Tokyo*, **62**, 347-365.

ISEZAKI, N., 1986, A magnetic anomaly map of the Japan Sea, *J. Geomag. Geolectr.*, 38, 403-410.

JAPANESE DELP RESEARCH GROUP ON BACK-ARC BASINS, 1987, Report on DELP 1985 cruises in the Japan Sea Part I: General outline, *Bull. Earthq. Res. Inst., Univ. Tokyo.*, **62**, 339-346.

KANEOKA, I., 1986, Constraints on the time of the evolution of the Japan Sea floor

based on radiometric ages, *J. Geomag. Geoelectr.*, 38, 475-485.

KASAHARA, J., M. TAKAHASHI, T. MATSUBARA and M. KOMIYA, 1985, Mass storage digital ocean bottom seismometer and hydrophone (DOBSH) controlled by micro-processors using ADPCM voice synthesizing, *Bull Earthq. Res. Inst., Univ. Tokyo*, **60**, 23-37.

KATAO, H., Y. KITAHARA and N. ISEZAKI, 1985, Measurement of the three components of the geomagnetic field, in Preliminary reports of the Hakuho Maru cruise KH84-1, ed. by K. Kobayashi, Ocean Res. Inst. Univ. Tokyo, pp. 10-25.

KIMURA, M., T. MATSUDA, H. SATO, I. KANEOKA, H. TOKUYAMA, N. ISEZAKI, S. KURAMOTO, A. OSHIDA, K. SHIMAMURA, K. TAMAKI, H. KINOSHITA, S. UYEDA and K. KAWABATA, 1987, Report on DELP 1985 cruises in the Japan Sea Part VII: Topography and geology of the Yamato Basin and its vicinity, *Bull. Earthq. Res. Inst., Univ. Tokyo.*, **62**, 447-484.

KOBAYASHI, K. and N. ISEZAKI, 1976, Magnetic anomalies in Japan Sea and Shikoku Basin and their possible tectonic implications, in The geophysics of the Pacific Ocean Basin and its margin, Geophys. Monogr. Ser., 19, ed. by G.H. Sutton et al., AGU, Washington, D.C., pp. 235-251.

LUDWIG, W.J., S. MURAUCHI and R.E. HOUTZ, 1975, Sediments and structure of the Japan Sea, *Geol. Soc. Amer. Bull.*, **87**, 651-664.

MATSUDA, T. and S. UYEDA, 1971, On the Pacific-type orogeny and its model, Tectonophys., **11**, 5-27.

MCCLAIN, J.S. and C.A. ATALIAH, 1986, Thickning of the oceanic crust with age, *Geology*, **14**, 574-576.

MIYASHIRO, A., 1986, Hot regions and the origin of marginal basins in the western Pacific, *Tectonophys.*, **122**, 195-216.

MROZOWSKI, C.L. and D.E. HAYES, 1979, The evolution of the Palace Vele Bsin, Eastern Philippine Sea, *Earth Planet. Sci. Lett.*, **46**, 49-67.

MURAUCHI, S., 1966, Explosion seismology, in Second Progress Report on the Upper Mantle Project of Japan (1965-1966), Natl. Committee for UMP, Sci. Council of Japan, pp. 11-13.

MURAUCHI, S., 1971, The renewal of island arcs and the tectonics of marginal seas, in Island arc and marginal sea, ed. by S. Asano and G.B. Udintsev, Tokai Univ. Press., pp. 39-56 (in Japanese).

MURAUCHI, S., 1972, Crustal structure in the Sea of Japan from seismic exploration, *Kagaku*, **42**, 367-375 (in Japanese).

MURAUCHI, S., N. DEN, S. ASANO, H. HOTTA, T. YOSHII, T. ASANUMA, K. HAGIWARA, K. ICHIKAWA, T. SATO, W.J. LUDWIG, J.I. EWING, N.T. EDGER and R.E. HOUTZ, 1968, Crustal structure of the Philippine Sea, *J. Geophys. Res.*, **73**, 3143-3171.

MUTTER, J.C., W.R. BUCK and C.M. ZEHNDER, 1988, Convective partial melting 1. a model for the formation of thick basaltic sequences during the initiation of spreading, *J. Geophys. Res.*, **93**, 1031-1048.

NAGUMO, S., H. KINOSHITA, J. KASAHARA, T. OUCHI, H. TOKUYAMA, T. ASANUMA, S. KORESAWA and H. AKIYOSHI, 1986, Report on DELP 1984 cruises in the Middle Okinawa Trough Part II: Seismic structure studies, *Bull. Earthq. Res. Inst., Univ. Tokyo*, **61**, 167-202.

OKADA, H., T. MORIYA, T. MASUDA, T. HASEGAWA, S. ASANO, K. KASAHARA, A. IKAMI, H. AOKI, Y. SASAKI, N. HURUKAWA and K. MATSUMURA, 1978, Velocity anisotropy in the Sea of Japan as revealed by big explosions, *J. Phys. Earth*, **26**, 491-502.

OTOFUJI, Y., A. HAYASHIDA and M. TORII, 1985, When was the Japan Sea opened?: paleomagnetic evidence from Southwest Japan, in Formation of active ocean margins, ed. by N. Nasu *et al.*, TERRAPUB, Tokyo, pp. 551-556.

OTOFUJI, Y., T. MATSUDA and S. NOHDA, 1986, Brief review of miocene opening of the Japan Sea: paleomagnetic evidence from the Japan Arc, *J. Geomag. Geoelectr.*, 38,

287-294.

RAITT, R. W., 1963, The crustal rocks, in The Sea, vol. 3, ed. by M. N. Hill, pp. 85-102, Wiley-Interscience, New York.

SAYANAGI, K., N. ISEZAKI and Y. KITAHARA, 1987, Report on DELP 1985 cruises in the Japan Sea Part IV: Geomagnetic anomalis over the Seamounts in the Yamato Basin, *Bull. Earthq. Res. Inst., Univ. Tokyo.*, **62**, 391-416.

SHOR, G. G., JR., H. W. MENARD and R. W. RAITT, 1970, Structure of the Pacific basin, in The Sea, vol. 4, part 2, ed. by A. E. Maxwell, pp. 3-27, Wiley-Interscienec, New York.

SPUDICH, P. and J. ORCUTT, 1980, A new look at the seismic velocity structure of the oceanic crust, *Rev. Geophys. Space Phys.*, **18**, 627-645.

SUYEMASU, M., 1988, Precise P-wave velocity structure analysis of the Yamato Basin, Japan Sea, M. Sc. thesis Chiba Univ. (in Japanese).

TAKAHASHI, M., 1986, Arc volcanism around the opening of the Japan Sea, *Kagaku*, **56**, 103-111 (in Japanese).

TAKEUCHI, A., 1986, Oligocene/miocene rotational blockmovement and paleostress field of Japan, *J. Geomag. Geoelectr.*, **38**, 495-511.

TALANDIER, J. and E. A. OKAL, 1987, Crustal structure in the Society and Tuamotu Islands, French Polynesia, *Geophys. J. R. astr. Soc.*, **88**, 499-528.

TALWANI, M., J. L. WORZEL and M. LANDISMAN, 1959, Rapid gravity computation for two-dimensional bodies with application to the Mendocino Submarine Fracture Zone, *J. Geophys. Res.*, **64**, 49-59.

TAMAKI, K., 1986, Age estimation of the Japan Sea on the basis of stratigraphy, basement depth, and heat flow data, *J. Geomag. Geoelectr.*, **38**, 427-446.

TAYLOR, B. and G. D. KARNER, 1983, On the evolution of marginal basins, *Rev. Geophys. Space Phys.*, **21**, 1727-1741.

TERADA, T., 1934, On the bathymetrical features of the Japan Sea, *Bull. Earthq. Res. Inst., Univ. Tokyo*, **12**, 650-656.

TOKUYAMA, H., M. SUYEMASU, K. TAMAKI, E. NISHIYAMA, S. KURAMOTO, K. SUYEHIRO, H. KINOSHITA and A. TAIRA, 1987, Report on DELP 1985 cruises in the Japan Sea Part III: Seismic reflection studies in the Yamato Basin and Yamato Rise Area, *Bull. Earthq. Res. Inst., Univ. Tokyo.*, **62**, 367-390.

TOMODA, Y., 1973, Maps of Free air and Bouguer gravity anomalies in and around Japan, Univ. Tokyo Press.

UYEDA, S. and H. KANAMORI, 1979, Back-arc opening and the mode of subduction, *J. Geophys. Res.*, **84**, 1049-1061.

WATTS, A. B., U. S. TEN BRINK, P. BUHL and T. M. BROCHER, 1985, A multichannel seismic study of lithospheric flexure across the Hawaiian-Emperor seamount chain, *Nature*, **315**, 105-111.

YASKAWA, K., 1975, Paleolatitude and relative position of Southwest Japan and Korea in the Cretaceous, *Geophys. J. R. astr Soc.*, **43**, 835-846.

大和海盆の地震波構造とその形成過程

地震研究所　片　尾　浩

1985年の DELP 航海では日本海大和海盆において屈折法地震探査が行なわれた．測線 A (NE-SW, 230 km) およびこれと直交する測線 B (NW-SE, 130 km) 上に 20 台の海底地震計を配置し，エアガン，総計 5 トンの火薬を人工震源として用いた．本研究ではこのとき得られたデータを基に大和海盆の地殻および上部マントルの精密な地震波速度構造を求め，同海盆の形成過程を考察する．

両測線の記録断面を比較すると，Pn が初動として始めて出現する距離，およびモホ面からの臨界反射とみられる相の到達距離に系統的な差異が認められる．これらのことは，南東—北西方向に速く東西—北東方向に遅い P 波速度異方性が上部マントルに存在することを示している．

詳しい構造解析は 2 次元波線追跡法による理論走時および理論波形と観測波形を比較し，試行錯誤をくりかえしてモデリングをおこなった．重力異常の観測値と矛盾しない解としては，モホ面の深さ 16.5 km で両測線ともにほぼ平坦なモホ面を持ち，Pn 速度は測線 AB 各々 7.65 km/s および 8.3 km/s となるモデルが最も適当であると思われる．この他にも，理論走時を観測走時に0.1 秒以内の精度で合わせ，理論記象も観測波形をほぼ満足するモデルとしては，測線交点におけるモホ面の深さ 16 km から 18 km の範囲で，測線 B に沿ったモホ面の形状および下部地殻の速度勾配等を変えることによって，多様な解が存在し得る．しかし，重力異常を満足するためには深さ 17 km 以浅でほぼ平坦なモホ面の形状が要求される．

上述のモデルはいずれも地殻上部で速度が連続的に大きな速度勾配で増加し，地殻下部には 7.0 km/s 前後で速度勾配の小さい海洋第 3 層に相当する層が存在するなど，速度分布に関しては典型的な海洋性地殻の特徴を備えている．しかし，地殻の厚さは 13～15 km で，通常の海洋地殻の 2 倍近くに達する特異なものである．

約 15 Ma の古地磁気偏角の急激な変化は，大和海盆のこの時期の急激な拡大によってもたらされたと考えられる．異常に厚い地殻の形成は，このような拡大速度の下で未知の地殻形成メカニズムが働いたことによるのかもしれない．